How adherence to public health measures shapes epidemic spreading: A temporal network model

How adherence to public health measures shapes epidemic spreading: A temporal network model

Cite as: Chaos **31**, 043115 (2021); https://doi.org/10.1063/5.0041993
Submitted: 27 December 2020 . Accepted: 08 March 2021 . Published Online: 13 April 2021

Brandon M. Behring, **Alessandro Rizzo, and** **Maurizio Porfiri**

How adherence to public health measures shapes epidemic spreading: A temporal network model

Cite as: Chaos **31**, 043115 (2021); doi: 10.1063/5.0041993
Submitted: 27 December 2020 · Accepted: 8 March 2021 ·
Published Online: 13 April 2021

View Online Export Citation CrossMark

Brandon M. Behring,[1] Alessandro Rizzo,[2,3,a)] and Maurizio Porfiri[1,4,5,b)]

AFFILIATIONS

[1]Department of Mechanical and Aerospace Engineering, Tandon School of Engineering, New York University, Six MetroTech Center, Brooklyn, New York 11201, USA
[2]Department of Electronics and Telecommunications, Politecnico di Torino, 10128 Torino, Italy
[3]Office of Innovation, Tandon School of Engineering, New York University, Six MetroTech Center, Brooklyn, New York 11201, USA
[4]Department of Biomedical Engineering, Tandon School of Engineering, New York University, Six MetroTech Center, Brooklyn, New York 11201, USA
[5]Center for Urban Science and Progress, Tandon School of Engineering, New York University, 370 Jay Street, Brooklyn, New York 11201, USA

[a)]**Electronic mail:** alessandro.rizzo@polito.it
[b)]**Author to whom correspondence should be addressed:** mporfiri@nyu.edu

ABSTRACT

The COVID-19 pandemic has laid bare the importance of non-pharmaceutical interventions in the containment of airborne infectious diseases. Social distancing and mask-wearing have been found to contain COVID-19 spreading across a number of observational studies, but a precise understanding of their combined effectiveness is lacking. An underdeveloped area of research entails the quantification of the specific role of each of these measures when they are differentially adopted by the population. Pursuing this research allows for answering several pressing questions like: how many people should follow public health measures for them to be effective for everybody? Is it sufficient to practice social distancing only or just wear a mask? Here, we make a first step in this direction, by establishing a susceptible–exposed–infected–removed epidemic model on a temporal network, evolving according to the activity-driven paradigm. Through analytical and numerical efforts, we study epidemic spreading as a function of the proportion of the population following public health measures, the extent of social distancing, and the efficacy of masks in protecting the wearer and others. Our model demonstrates that social distancing and mask-wearing can be effective in preventing COVID-19 outbreaks if adherence to both measures involves a substantial fraction of the population.

COVID-19 vaccination is underway but our fight against this deadly virus is by no means over. There is widespread consensus in the public health community that social distancing and mask-wearing should be pursued for a long while, likely for the entirety of 2021. Despite these recommendations, not everybody wears a mask, and not everybody practices social distancing. What are the consequences of these choices made by some individuals on the health of all of us? Here, we establish a mathematical model to explore the combined effect of mask-wearing and social distancing by a fraction of the population on the spreading of COVID-19. The predictions of our mathematical model suggest that COVID-19 outbreaks can be prevented if a substantial fraction of the population adheres to both social distancing and mask-wearing. The success of these combined measures is demonstrated in the study of real-world data on COVID-19 in the USA. States that are suffering the most from the spreading are also those that fall well above the epidemic threshold predicted by our model, due to limited adherence to public health guidelines.

I. INTRODUCTION

Public health experts have long feared a highly contagious airborne pandemic[1] that would have the potential to cause mass casualties like the 1918 Spanish flu. The Centers for Disease Control and Prevention (CDC) has estimated that the 1918 Spanish flu pandemic infected about 500×10^6 people worldwide and took the life of 3%–5% of the world's population over 15 months.[2] In recent years, there have been several warning signs of a possible pandemic caused by a novel respiratory virus. Severe acute respiratory syndrome (SARS)[3] and the Middle East respiratory syndrome (MERS)[4] infected only 2519 people and 8098 people, respectively,[5,6] due to non-pharmaceutical interventions (NPIs) that prevented them from spreading globally. These close calls highlighted the importance of NPIs in containing the spread of novel viruses before pharmaceutical options could be available.

In the last year, NPIs have been used once again to prevent the spread of a deadly virus. On March 11, 2020, the World Health Organization (WHO) declared COVID-19 a pandemic. As of December 2020, COVID-19 has infected almost 70×10^6 people worldwide with over 1.5×10^6 attributed deaths.[7] COVID-19's primary modes of transmission are through droplets[8] and aerosols.[9,10] In addition to scientific breakthroughs in genetic sequencing, genomic surveillance enabling rapid contact tracing, vaccine rollout, antiviral drugs, and travel restrictions, the fight against COVID-19 relies on social distancing and masks.[11]

Social distancing has two components, keeping a safe physical distance between people and reducing the number of times people come into close contact. Public health policy can be used to enforce social distancing through prohibiting mass gatherings, enforcing quarantine, school closure, and stay-at-home orders, at the expense of mental health and productivity.[12–14] There exists comprehensive evidence of the benefits of social distancing in reducing the spread of the pandemic.[15] The data also strongly suggest that social distancing measures in March and April 2020 precipitated an early end to seasonal influenza in the Northern Hemisphere and prevented it in the Southern Hemisphere.[16,17] Along with empirical data, mathematical models have also been leveraged to demonstrate the benefits of social distancing in the fight against COVID-19,[18] across a wide range of approaches, spanning network theory,[19,20] compartmental modeling,[21] and agent-based modeling.[22,23]

In addition to social distancing, mask-wearing has been often proposed to be critical in the control of COVID-19.[24] Experiments have shown that surgical masks effectively reduce the spread of viral particles expelled from the wearer[25,26] and protect the wearer by reducing exposure to high viral loads.[27] Whether we compare COVID-19 spreading across different states in the USA or across different countries worldwide, there is evidence that government-mandated mask use and COVID-19 cases are strongly related.[28] Along with empirical observations, the efficacy of masks has been assessed through compartmental models based on systems of differential equations[21,29] or stochastic simulations,[30] computational schemes employing a next-generation matrix approach,[31] and heterogeneous bond percolation on static networks.[32]

Despite the overwhelming evidence in favor of social distancing and masks, a mathematically based understanding of their combined effect is lacking. Particularly elusive is the quantification of the specific role played by either of these NPIs when they are differentially adopted within a population. Here, we present a network model of COVID-19 spreading to dissect the role of masks and social distancing on the spread of the epidemic. Toward capturing the concurrent evolution of the network of contacts and epidemic dynamics, we adopt activity-driven networks (ADNs). Different from "connectivity-driven" models where the network topology drives interactions, ADNs are "activity-driven" in that the interactions are characterized by a constant activity potential sampled from a probability distribution.[33]

In the seminal work by Perra *et al.*,[33] ADNs were used to model susceptible–infected–susceptible (SIS) transmission. The results were later extended to include susceptible–infected–removed (SIR) transmission and vaccination strategies,[34] self-protective behaviors,[35] and complex progression models.[36] Within the study of COVID-19, ADNs have been employed to examine the effects of active and inactive quarantine within an SIR model.[20] Susceptible–exposed–infected–non-infected–removed (SEINR) transmission was integrated in an ADN to investigate the effects of social distancing and travel restrictions[19] during the first wave of the COVID-19 pandemic in Italy. Building on the success of these studies, here, we establish an ADN-based model of COVID-19 spreading in which only a fraction of the population adheres to social distancing and mask-wearing. For a susceptible–exposed–infected–removed (SEIR) model, we provide analytical insight into the epidemic threshold and gather numerical evidence on the long-term dynamics of the spreading. The specific contribution of this study to ADNs is the formulation and mathematical analysis of a sub-population model that can be used to examine heterogeneities in network dynamical systems with stochastically time-varying topology. Although the study is motivated by the ongoing COVID-19 pandemic, it can find application in different fields that have benefited from the use of ADNs, such as diffusion of innovation[37] and consensus problems.[38] The existence of threshold values emphasizes the importance of a high level of adherence to NPIs; whereby falling below the critical values can lead to drastically different outcomes in the dynamics of the system.

The rest of the paper is organized as follows. In Sec. II, we outline the proposed ADN-based model. In Sec. III, we conduct a linear stability analysis in the mean-field limit to determine a closed-form expression for the epidemic threshold. In Sec. IV, we present numerical results that help validate analytical predictions and shed light on the role of different control parameters. Therein, we also attempt at a state-level analysis of pandemic in the USA, using available data on the adoption of NPIs. Finally, in Sec. V, we summarize our main findings and provide avenues for further work.

II. EPIDEMIC MODELING WITH DIFFERENTIAL SOCIAL DISTANCING AND MASK-WEARING

A network model represents the population as a graph—a set of nodes and edges. Nodes represent the individuals in the population, and edges encode contacts between pairs of individuals. In this vein, contagion travels from a node to another via paths formed by potentially time-varying edges.[39] More concretely, we model the epidemic through a temporal network $\mathcal{G}_t$ of N nodes. Each node is associated with an individual in a discrete state $\{S, E, I, R\}$ depending on the

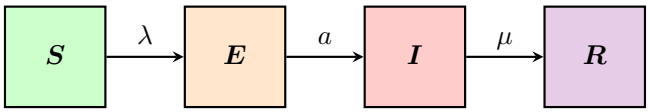

FIG. 1. Progression dynamics of an SEIR model, consisting of four compartments. An individual progresses from the susceptible state, *S*, to the exposed state, *E*, with a per-contact probability λ when interacting with an individual in the infected state *I*. The individual in the exposed state becomes infected, with a rate *a*. Finally, the individual's state changes to the removed state *R* with a rate μ.

individual's health status. An initially uninfected node begins in the susceptible state, *S*. At each time step Δt, if a node forms a connection with another node in the infected state, *I*, it enters the exposed state, *E*, with a per-contact probability λ. The parameter λ is modulated by the use of masks, which reduce the risk of transmission. The node remains in the exposed state for a latency period and enters the infected state with probability per unit time, or rate, $a > 0$. Finally, in the infected state, the node enters the removed state, *R*, with rate $\mu > 0$ (Fig. 1). The removed state encompasses individuals who are no longer susceptible to the infection. From the fraction of removed individuals, it is possible to resolve the number of individuals who are recovered and immunized and those who are dead, using fatality and recovery rates from the medical literature, similar to Ref. 19.

Each node $i \in \{1, 2, \ldots, N\}$ in the network is characterized by a time-independent, baseline activity potential x_i. Such an activity potential is defined as the ratio between the number of interactions made by the node and the total number of interactions made by all the nodes in the network during a fixed time interval, under the premise that no effort is made to practice social distancing. All the network's baseline activity potentials x_i are gathered in a vector $x \in \mathbb{R}^N$. Social distancing modulates the activity potentials, similar to the effect of masks on λ. The activity potentials x_i are independent and identically distributed realizations of a random variable. Following Refs. 33 and 34, we sample our random variable from a power-law distribution with exponent γ such that $2 < \gamma < 3$. A lower cutoff value of 10^{-3} is used when sampling from the distribution to avoid singularities. A power-law distribution is "fat-tailed"—this leads to an uneven distribution where a few highly active nodes are responsible for much of the network's contacts. This assumption has been empirically validated in real-world contact networks,[40,41] where most individuals have few interactions and only a few interact with many others.

As one might expect, the people who wear masks are also those who reduce their mobility (Fig. 2). In Fig. 2, we use data from the Institute for Health Metrics and Evaluation (IHME) at the University of Washington[42] to visualize the extent of mobility (inferred from cellphone mobility data) as a function of the fraction of a state's population who reports regularly wearing masks (using Facebook surveys). Pearson's correlation coefficient between the two variables is $r \approx -0.842$. Such a strong correlation suggests that the same people who reduce their mobility are also those who wear masks. We hypothesize that these mobility reductions are suggestive of practicing social distancing.

Specifically, based on this premise, we partition the population into two sub-populations (Fig. 3). Sub-population *A* consists of

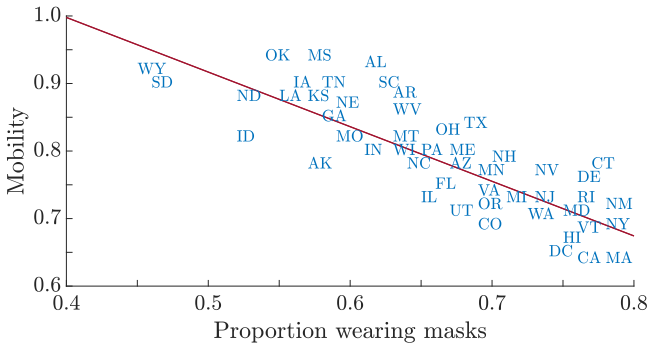

FIG. 2. Relationship between the proportion of people in each of the 50 USA states and the District of Columbia who regularly wear masks and their mobility compared to baseline averaged over the month of November 2020. The line identifies a least squares best fit line.

individuals who regularly wear masks and practice social distancing, and sub-population *B* comprises individuals whose behavior remains unchanged by the pandemic. This partition is implemented in our activity-driven network, $\mathcal{G}_t$, by assigning the nodes to two disjoint sets of cardinality N^A and N^B, such that $N = N^A + N^B$ is the total number of nodes in the network. Using an SEIR model for the coupled sub-populations, sub-population *A* is composed of S^A susceptible nodes, E^A exposed nodes, I^A infected nodes, and R^A removed nodes, which total to $N^A = S^A + E^A + I^A + R^A$. Similarly, we consider nodes in sub-population *B* as S^B, E^B, I^B, and R^B, where $N^B = S^B + E^B + I^B + R^B$.

Social distancing is included in the model by scaling the activity potentials in *A* by a positive factor $\eta < 1$. This implies that, at any time, the average number of active nodes in *A* is given by $\eta\langle x\rangle$, where $\langle\cdot\rangle$ defines the mean of a random variable. To incorporate the effect of mask-wearing, we introduce the parameters $\alpha_1, \alpha_2 \in [0, 1]$. The mask reduces the probability of an individual in sub-population *A* transmitting the virus by a factor of α_1 and the probability of getting

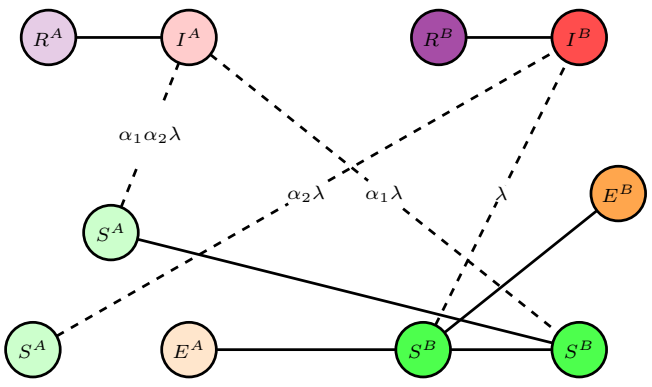

FIG. 3. Schematic of the proposed network model using two sub-populations. The dashed links represent possible pathways of contagion from I^A or I^B to either of S^B or S^A, along with the corresponding per-contact probability.

infected by α_2, thereby incorporating empirical observations on the function of masks[11] ($\alpha_1 = 1$ and $\alpha_2 = 1$ implies no effect of masks). In the literature, there is no consensus on the extent of protection offered by masks.[43,44] However, it is tenable to assume that the reduction in the probability of the mask wearer to transmit the virus is much more significant than the reduction in the probability of the mask wearer to get infected,[11,45,46] that is, $\alpha_2 > \alpha_1$. Parameters α_1, α_2, and η should be regarded as mathematical proxies for the considered public health measures within the proposed ADN-based model.

Initializing a disconnected network of $N = N^A + N^B$ nodes, the progression of the contagion on the network evolves according to the following rules:

(1) With probability $\eta x_i \Delta t$, each node i in A becomes active and generates m links that connect i to m other randomly selected nodes from the total network, $\mathcal{G}_t$. With probability $x_i \Delta t$, each node i in B becomes active and generates m links that connect to m other randomly selected nodes from the total network, $\mathcal{G}_t$.
(2) The SEIR model rules are run on the graph.
  (a) There are four ways an infected and susceptible node can interact:
    (i) If an infected node in A links with a susceptible node in A, the susceptible node becomes exposed with a per-contact transmission probability $\alpha_1\alpha_2\lambda$.
    (ii) If an infected node in A links with a susceptible node in B, the susceptible node becomes exposed with a per-contact transmission probability $\alpha_1\lambda$.
    (iii) If an infected node in B links with a susceptible node in A, the susceptible node becomes exposed with a per-contact transmission probability $\alpha_2\lambda$.
    (iv) If an infected node in B links with a susceptible node in B, the susceptible node becomes exposed with a per-contact transmission probability λ.
  (b) A node in the exposed state transitions to the infected state with a rate of a.
  (c) An infected node enters the removed state with a rate of μ.
(3) At the next time step $t + \Delta t$, all the edges in the network are deleted and the process resumes from step 1.

III. ANALYTICAL COMPUTATION OF THE EPIDEMIC THRESHOLD

In previous studies,[33,34] it was shown that, for both SIS and SIR epidemic models on an ADN with per-contact infection probability λ, baseline activity-potential vector x with first and second statistical moments $\langle x\rangle$ and $\langle x^2\rangle$, respectively, and recovery rate μ, the epidemic threshold is given in terms of the reproduction number[47] $\tilde{R}_0 = \frac{2m\lambda\langle x\rangle}{\mu}$. The inequality

$$\tilde{R}_0 > \tilde{R}_0^c := \frac{2\langle x\rangle}{\langle x\rangle + \sqrt{\langle x^2\rangle}} \tag{1}$$

sets up the condition for the inception of an epidemic outbreak. Therein, the superscript "c" is used to indicate the critical value of the reproduction number above which an exponential growth of infection cases occurs. Letting

$$R_0 := \frac{\tilde{R}_0}{\tilde{R}_0^c} = \frac{m\lambda}{\mu}\left(\langle x\rangle + \sqrt{\langle x^2\rangle}\right), \tag{2}$$

an outbreak occurs if $R_0 > 1$ and the infection dies off if $R_0 < 1$. In the following, we recover an equivalent result for an SEIR model and for the proposed network model in the limit cases where NPIs are absent or totally ineffective.

A. Governing equations

Here, we extend the SIR/SIS computations to the proposed model of COVID-19 spreading with differential social distancing and mask-wearing. For large N^A and N^B, we consider ${S^A}_x(t)$, ${E^A}_x(t)$, ${I^A}_x(t)$, ${R^A}_x(t)$ and ${S^B}_x(t)$, ${E^B}_x(t)$, ${I^B}_x(t)$, ${R^B}_x(t)$ to be the number of nodes in A and B with activity potential x at a time t (also referred to as "activity class x" in what follows) for the corresponding susceptible, exposed, infected, and removed compartments. Since a node cannot switch from sub-population A to B or from B to A, the number of nodes in A and B with activity level x, ${N^A}_x$ and ${N^B}_x$, remain constant and are given by

$${N^A}_x = {S^A}_x + {E^A}_x + {I^A}_x + {R^A}_x, \tag{3a}$$

$${N^A}_x = {S^B}_x + {E^B}_x + {I^B}_x + {R^B}_x. \tag{3b}$$

The proportion of nodes in A is defined as $\beta = \frac{N^A}{N}$.

Once infected, a node becomes exposed, and it moves to the infected class at a rate given by $a > 0$. The transmission reduction from masks is incorporated in the scaling parameters α_1 and α_2 and social distancing is implemented on sub-population A through the scaling parameter η.

In the mean-field approximation ($N \to \infty$), the number of nodes in sub-population A in the exposed state and activity class x at a time $t + \Delta t$ is given by

$$\begin{aligned}
{E^A}_x(t+\Delta t) = {E^A}_x(t) - a{E^A}_x(t)\Delta t &+ \alpha_1\alpha_2\beta m\lambda\left({N^A}_x - {E^A}_x(t) - {I^A}_x(t) - {R^A}_x(t)\right)\eta x\int \mathrm{d}\tilde{x}\frac{{I^A}_{\tilde{x}}(t)}{N^A}\Delta t \\
&+ \alpha_1\alpha_2\beta m\lambda\left({N^A}_x - {E^A}_x(t) - {I^A}_x(t) - {R^A}_x(t)\right)\int \mathrm{d}\tilde{x}\tilde{x}\frac{\eta{I^A}_{\tilde{x}}(t)}{N^A}\Delta t \\
&+ \alpha_2(1-\beta)m\lambda\left({N^A}_x - {E^A}_x(t) - {I^A}_x(t) - {R^A}_x(t)\right)\eta x\int \mathrm{d}\tilde{x}\frac{{I^B}_{\tilde{x}}(t)}{N^B}\Delta t \\
&+ \alpha_2(1-\beta)m\lambda\left({N^A}_x - {E^A}_x(t) - {I^A}_x(t) - {R^A}_x(t)\right)\int \mathrm{d}\tilde{x}\tilde{x}\frac{{I^B}_{\tilde{x}}(t)}{N^B}\Delta t.
\end{aligned} \tag{4}$$

In Eq. (4), the first term refers to exposed individuals of class x in A at the previous time step. The second term accounts for exposed nodes of class x in A that transition from the exposed to the infected state I^A, after the latency period. The third term identifies active susceptible individuals of class x in A that become exposed by interacting with an infected node in A from any activity class; note the presence of the factor $\alpha_1\alpha_2$ to account for the reduction in transmission and increased protection by the wearer, along with η to specify social distancing. The fourth term is similar to the third, but it relates to any susceptible node in class x, active or not, that contracts the infection from any active infected node in A. The fifth and sixth terms duplicate the mechanism of the third and fourth terms, respectively, to transmission between the two sub-populations; note that, in this case, we only have the factor α_2 to capture the protection offered by masks to susceptible nodes in A.

The number of nodes in sub-population A in the infected state and activity class x is

$$I^A{}_x(t+\Delta t) = I^A{}_x(t) + aE^A{}_x(t)\Delta t - \mu I^A{}_x(t)\Delta t. \tag{5}$$

In Eq. (5), the number of infected nodes in A increases when an exposed node in A becomes infected after a latency period and it decreases when an infected node in A enters the removed state.

Similarly, the number of nodes in B in the exposed state and activity class x at a time $t+\Delta t$ in the mean-field approximation is given by

$$\begin{aligned} E^B{}_x(t+\Delta t) = {} & E^B{}_x(t) - aE^B{}_x(t)\Delta t + (1-\beta)m\lambda\left(N^B{}_x - E^B{}_x(t) - I^B{}_x(t) - R^B{}_x(t)\right)x\int \mathrm{d}\tilde{x}\frac{I^B{}_{\tilde{x}}(t)}{N^B}\Delta t \\ & + (1-\beta)m\lambda\left(N^B{}_x - E^B{}_x(t) - I^B{}_x(t) - R^B{}_x(t)\right)\int \mathrm{d}\tilde{x}\tilde{x}\frac{I^B{}_{\tilde{x}}(t)}{N^B}\Delta t \\ & + \alpha_1\beta m\lambda\left(N^B{}_x - E^B{}_x(t) - I^B{}_x(t) - R^B{}_x(t)\right)x\int \mathrm{d}\tilde{x}\frac{I^A{}_{\tilde{x}}(t)}{N^A}\Delta t \\ & + \alpha_1\beta m\lambda\left(N^B{}_x - E^B{}_x(t) - I^B{}_x(t) - R^B{}_x(t)\right)\int \mathrm{d}\tilde{x}\tilde{x}\frac{\eta I^A{}_{\tilde{x}}(t)}{N^A}\Delta t, \end{aligned} \tag{6}$$

and the number of nodes in B in the infected state and activity class x is

$$I^B{}_x(t+\Delta t) = I^B{}_x(t) + aE^B{}_x(t)\Delta t - \mu I^B{}_x(t)\Delta t. \tag{7}$$

Terms in Eqs. (6) and (7) have analogous interpretations as those in Eqs. (4) and (5). The key difference is the lack of the factors α_2 and η due to the lack of social distancing and protection from mask-wearing in sub-population B.

The evolution of the removed state in the two sub-populations is simply

$$R^A{}_x(t+\Delta t) = R^A{}_x(t) + \mu I^A{}_x(t)\Delta t, \tag{8a}$$

$$R^B{}_x(t+\Delta t) = R^B{}_x(t) + \mu I^B{}_x(t)\Delta t. \tag{8b}$$

B. First-order equations

Here, we provide an analytical expression for the epidemic threshold as a function of all the control parameters. Toward this aim, we assume that, initially, there are no nodes in the removed state for all activity classes, that is, $R^A{}_x(0) = R^B{}_x(0) = 0$ for all x.

To perform this analysis, we work with sub-population-wide quantities that consolidate epidemic spreading across different activity classes. Specifically, we deal with the sub-population-wide numbers of infected and exposed individuals over all activity classes, namely,

$$I^A = \int I^A{}_x\,\mathrm{d}x, \tag{9a}$$

$$I^B = \int I^B{}_x\,\mathrm{d}x, \tag{9b}$$

$$E^A = \int E^A{}_x\,\mathrm{d}x, \tag{9c}$$

$$E^B = \int E^B{}_x\,\mathrm{d}x, \tag{9d}$$

along with first-order moments, obtained by multiplying by x and integrating, that is,

$$\theta^A = \int xI^A{}_x\,\mathrm{d}x, \tag{10a}$$

$$\theta^B = \int xI^B{}_x\,\mathrm{d}x, \tag{10b}$$

$$\psi^A = \int xE^A{}_x\,\mathrm{d}x, \tag{10c}$$

$$\psi^B = \int xE^B{}_x\,\mathrm{d}x. \tag{10d}$$

Integrating both sides of Eqs. (4)–(7) over all activity classes and retaining only first-order terms yield

$$\frac{\mathrm{d}I^A}{\mathrm{d}t} = -\mu I^A + aE^A, \tag{11a}$$

$$\frac{dI^B}{dt} = -\mu I^B + aE^B, \tag{11b}$$

$$\frac{dE^A}{dt} = -aE^A + \alpha_1\alpha_2\beta m\lambda\eta\left(\langle x\rangle I^A + \theta^A\right) + \alpha_2\beta m\lambda\left(\eta\langle x\rangle I^B + \theta^B\right), \tag{11c}$$

$$\frac{dE^B}{dt} = -aE^B + (1-\beta)m\lambda\left(\langle x\rangle I^B + \theta^B\right) + \alpha_1(1-\beta)m\lambda\left(\langle x\rangle I^A + \eta\theta^A\right), \tag{11d}$$

as $\Delta t \to 0$.

Likewise, by multiplying both sides of (4)–(7) by x, and then integrating over all activity classes and keeping only first-order terms gives

$$\frac{d\theta^A}{dt} = -\mu\theta^A + a\psi^A, \tag{12a}$$

$$\frac{d\theta^B}{dt} = -\mu\theta^B + a\psi^B, \tag{12b}$$

$$\frac{d\psi^A}{dt} = -a\psi^A + \alpha_1\alpha_2\beta m\lambda\eta\left(\langle x^2\rangle I^A + \langle x\rangle\theta^A\right) + \alpha_2\beta m\lambda\left(\eta\langle x^2\rangle I^B + \langle x\rangle\theta^B\right), \tag{12c}$$

$$\frac{d\psi^B}{dt} = -a\psi^B + (1-\beta)m\lambda\left(\langle x^2\rangle I^B + \langle x\rangle\theta^B\right) + \alpha_1(1-\beta)m\lambda\left(\langle x^2\rangle I^A + \eta\langle x\rangle\theta^A\right), \tag{12d}$$

as $\Delta t \to 0$.

To examine the stability of the system of linear differential equations in equation sets (11) and (12), we introduce

$$z = \left[I^A, I^B, \theta^A, \theta^B, E^A, E^B, \psi^A, \psi^B\right]^{\mathsf{T}}, \tag{13}$$

where T indicates matrix transposition. Hence, we can formulate the problem in the form $\frac{dz}{dt} = Jz$, where J is a 8×8 state matrix for the linearized dynamical system.

All the eigenvalues of J are real, and the stability of the infection-free state is controlled by the largest eigenvalue of J, $\Lambda_{\max}$, which can be written as

$$\Lambda_{\max} = -m\mu\lambda + m\lambda f_1(\alpha_1,\alpha_2,\beta,\eta)\langle x\rangle + m\lambda f_2(\alpha_1,\alpha_2,\beta,\eta)\sqrt{\langle x^2\rangle}, \tag{14}$$

where

$$f_1(\alpha_1,\alpha_2,\beta,\eta) := 1 - \beta + \alpha_1\alpha_2\eta\beta, \tag{15a}$$

$$f_2(\alpha_1,\alpha_2,\beta,\eta) := \sqrt{(1-\beta+\alpha_1\alpha_2\eta^2\beta)\,(1-\beta+\alpha_1\alpha_2\beta)}. \tag{15b}$$

An epidemic outbreak occurs if $\Lambda_{\max} > 0$, so that the infection-free state is unstable above the epidemic threshold, given by

$$\frac{m\eta\lambda}{\mu} > \frac{1}{f_1(\alpha_1,\alpha_2,\beta,\eta)\langle x\rangle + f_2(\alpha_1,\alpha_2,\beta,\eta)\sqrt{\langle x^2\rangle}}. \tag{16}$$

C. Limit cases

Here, we specialize our general expression of the epidemic threshold in Eq. (16) to several limit cases. If there is no social distancing even in sub-population A, then $\eta = 1$ and Eq. (16) can be written as a scaled version of the critical reproduction number from Eq. (1), in the absence of interventions. Specifically, we obtain

$$\tilde{R}_0 > f(\alpha_1,\alpha_2,\beta)\tilde{R}_0^c, \tag{17}$$

where

$$f(\alpha_1,\alpha_2,\beta) := \frac{1}{1-\beta\,(1-\alpha_1\alpha_2)} \tag{18}$$

and $\tilde{R}_0^C$ is the critical reproduction number, defined by Eq. (1), in the absence of interventions. This result is consistent with expectations for the following cases:

1. If masks bring no benefit ($\alpha_1 = \alpha_2 = 1$) or the behavior of the entire population is unchanged ($\beta = 0$), then $f(\alpha_1,\alpha_2,\beta) = 1$. This case, therefore, coincides with the original incarnation of an SEIR model over an ADN. Consistently, the threshold reduces to the result in Ref. 33.
2. If all nodes are in sub-population A ($\beta = 1$), then $f(\alpha_1,\alpha_2,1) = \frac{1}{\alpha_1\alpha_2}$, thereby indicating that the epidemic outbreak can be greatly suppressed by wearing efficacious masks.
3. If the masks completely prevent transmission in either direction ($\alpha_1 = 0$ or $\alpha_2 = 0$), then the sub-population that adheres to mask-wearing is virtually not part of the disease transmission. In fact, $f(0,0,\beta) = \frac{1}{1-\beta}$, which yields the same threshold as the case in which a proportion β of the population is randomly vaccinated.[34]
4. The analysis is simplified in the symmetric case where $\alpha = \alpha_1 = \alpha_2$. In Fig. 4, we plot the function in Eq. (18) for $\alpha \in [0.5, 1.0]$ and $\beta \in [0, 1]$. Contour curves are suggestive of a substitute action between adherence to mask-wearing and their effectiveness, such that the same value of the function can be obtained through different combinations of the parameters. A shadowed area in the α–β plane highlights the most plausible parameter space for adherence and effectiveness, as observed in Refs. 11, 26, 28, 29, 31, 42, and 44.

IV. NUMERICAL RESULTS

Here, we present a detailed numerical study to corroborate our analytical expression for the epidemic threshold in Eq. (16), characterize the long-term outcome of the outbreak (in terms of steady-state fraction of removed individuals), and highlight the connection between our model and real-world observations. In all simulations, we implement an ADN of size $N = 10^6$, with a number of connections per active node of $m = 20$ and a decay rate for the power-law activity distribution of $\gamma = -2.1$ with cutoffs set at $[10^{-3}, 1]$. Simulations are run with a time step of $\Delta t = 0.5$ day. A small fraction of $0.01N$ random individuals is infected at the onset of each simulation, and 100 realizations are utilized when computing averages.

Key epidemiological parameters of the model are borrowed from Ref. 19; in particular, we implement the SEIR model with a recovery rate of $\mu = 0.2\,\text{day}^{-1}$ and a latency time $a = 0.5\,\text{day}^{-1}$.

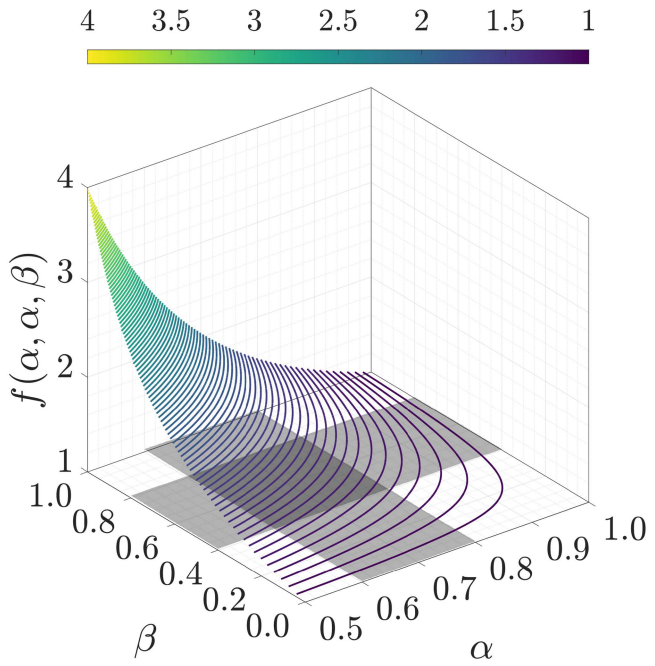

FIG. 4. Visualization of function $f(\alpha_1, \alpha_2, \beta)$ in Eq. (18) in the symmetric case where $\alpha = \alpha_1 = \alpha_2$. The shadowed region highlights the most plausible parameter region.

Instead of utilizing the per-contact infection rate, λ, as a control parameter, we choose to work with the reproduction rate, R_0, which can be obtained from Eq. (2) using the given values of m, γ, and μ. A meta-analysis of the early days of the COVID-19 pandemic[48] suggests that, before interventions, the observed reproduction rate, R_0, was likely between 2 and 3 but could be as high as 4. In our study, we treat R_0 as a continuous control parameter between 1 and 4.

Borrowing again from Ref. 19, we consider three values for the reduction in activity due to social distancing ($\eta = 0.25$, $\eta = 0.5$, and $\eta = 0.75$) toward capturing the extrema of severe and modest social distancing. Since the net efficacy of masks is still debated,[43] we conduct our analysis using values on the optimistic ($\alpha_1 = 0.25$ and $\alpha_2 = 0.75$) and the pessimistic ($\alpha_1 = 0.5$ and $\alpha_2 = 1$) ends of the spectrum examined in the literature.[11,26,28,29,31,44] The optimistic end of the spectrum pertains to the use of N95 respirators and likely overestimate the efficacy of surgical masks.[26] The last control parameter we examine is the proportion of individuals following public health guidelines and social distancing, β. We treat this as a continuous control parameter between 0 and 1; for reference, β should vary between $\beta = 0.4$ and $\beta = 0.8$ in November 2020 in the USA (Fig. 2).

We perform four parametric studies, in which we compute the steady-state proportion of the total population R^∞/N who eventually enters the removed state as a function of β and R_0. The first two studies seek to isolate the specific benefits of either social distancing or mask-wearing. To ascertain the role of social distancing alone, we focus on the case of severe social distancing ($\eta = 0.25$), in the absence of beneficial effects of masks ($\alpha_1 = \alpha_2 = 1$). Similarly, we examine the role of mask-wearing alone using optimistic assumptions on mask efficacy ($\alpha_1 = 0.25$ and $\alpha_2 = 0.75$) and discarding social distancing ($\eta = 1$). The next two scenarios seek to understand the combined effect of mask-wearing and social distancing under pessimistic and optimistic assumptions. First, we consider the case of moderate social distancing ($\eta = 0.75$), along with a pessimistic assumption on the efficacy of masks ($\alpha_1 = 0.5$ and $\alpha = 1$). Finally, we study the case of intermediate social distancing ($\eta = 0.5$) with an optimistic assumption on mask efficacy ($\alpha_1 = 0.25$ and $\alpha = 0.75$) to illustrate an achievable scenario under the use of N95 respirators.

After exploring these four scenarios, we turn to real-world data on the epidemic in the USA to understand which of the states is below or above the epidemic threshold, according to our theoretical predictions in Eq. (16). We perform the analysis using different values of R_0, and for each state, we utilize available data on mask-wearing and social distancing (Fig. 2). Upon gathering insight into each of the states, we perform a statistical analysis against real data on infection to offer partial support in favor of the proposed modeling approach.

A. Parametric studies

We first consider the scenario where severe social distancing is undertaken ($\eta = 0.25$) without mask-wearing [Fig. 5(a)]. Numerical results confirm the existence of a threshold in the parameter space, below which the epidemic dies out in time and the fraction of removed individuals approaches zero. Our theoretical prediction of the epidemic threshold from Eq. (16) is in excellent agreement with numerical results. Minor discrepancies are due to the time-discrete nature of the simulation that is executed at a finite time resolution. For $\beta = 0$, the threshold value for the reproduction rate is $R_0 = 1$ and then it increases nonlinearly with β, reaching a value close to 4.

This finding indicates that the higher R_0 is, the larger should be the fraction of the population who practice social distancing to prevent an epidemic outbreak. For example, for $R_0 = 2$, it is sufficient that $\beta = 0.8$ to contain the epidemic, while for $R_0 = 4$, we need almost the entire population to practice social distancing if no other NPI beyond the two considered herein is implemented. Thus, in the USA, where a large fraction of the population does not comply with public health measures (Fig. 2), social distancing alone cannot suffice to contain the epidemic. These predictions are robust with respect to moderate variations of model parameters, as shown in the Appendix.

On the opposite side of the spectrum of NPIs, we examine the scenario where masks are very effective in reducing transmission and increasing protection ($\alpha_1 = 0.25$ and $\alpha_2 = 0.75$), but social distancing is not practiced [Fig. 5(b)]. As expected, our numerics align with our analytical prediction of the epidemic threshold, and we highlight the inadequacy of a single control measure to combat the pandemic. For example, for $R_0 = 2$, we would require at least a fraction $\beta = 0.6$ to wear a highly efficacious mask for containing the epidemic, and this fraction should increase to $\beta = 0.9$ for $R_0 = 4$.

Combining the two control measures could, in principle, help reduce the fraction of individuals who need to adhere to public health measures. However, the effectiveness of a combined approach depends on the efficacy of the masks and the extent to which social

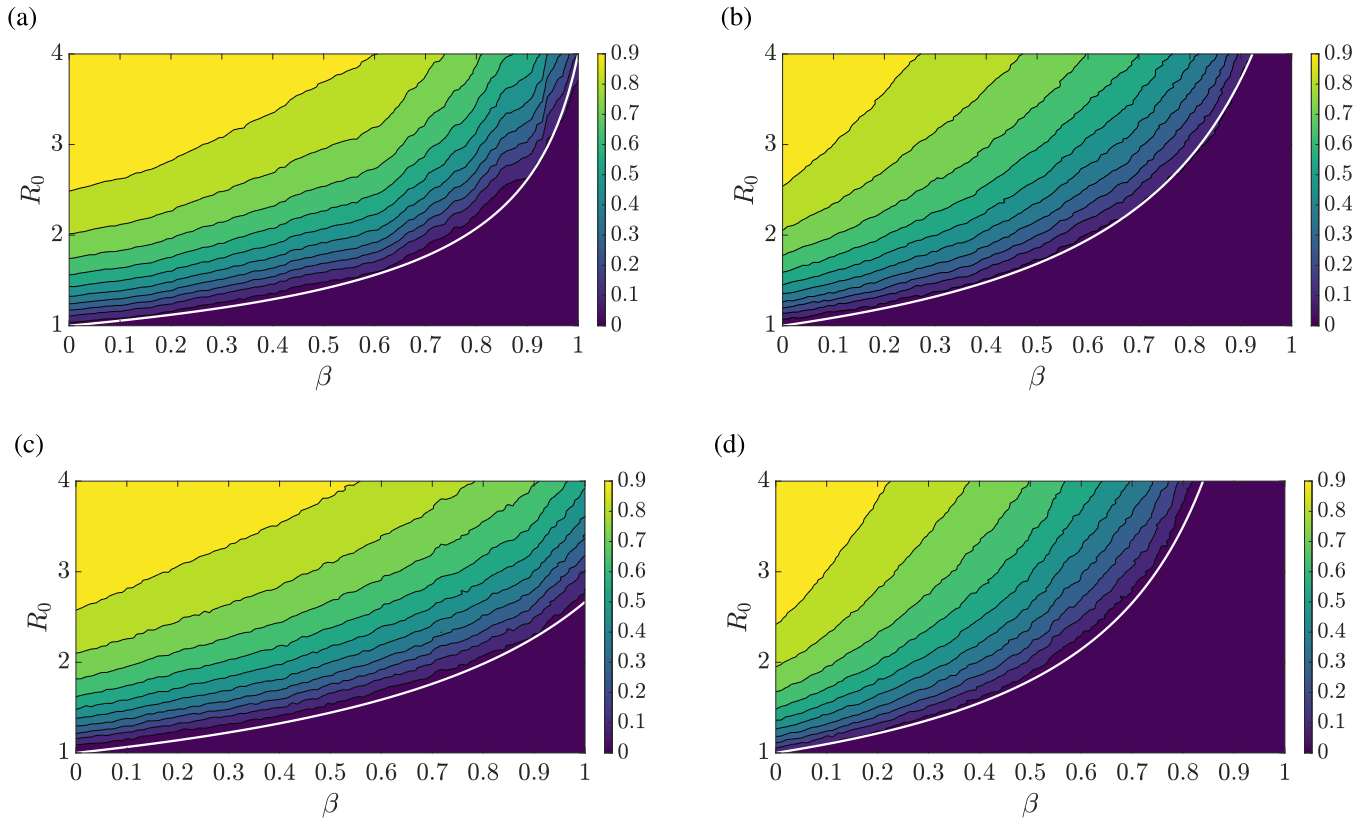

FIG. 5. Steady-state fraction of removed individuals, R^{∞}/N (color coded), as a function of the proportion of the population who comply with public health measures, β, and reproduction rate, R_0. The white line is the epidemic threshold computed using Eq. (16). (a) Severe social distancing and no mask-wearing; (b) no social distancing and high effectiveness of masks; (c) moderate social distancing, masks reducing transmission but not offering self-protection; (d) intermediate social distancing and high effectiveness of masks. (a) $\eta = 0.25$, $\alpha_1 = 1$, and $\alpha_2 = 1$, (b) $\eta = 1$, $\alpha_1 = 0.25$, and $\alpha_2 = 0.75$, (c) $\eta = 0.75$, $\alpha_1 = 0.5$, and $\alpha_2 = 1$, and (d) $\eta = 0.5$, $\alpha_1 = 0.25$, and $\alpha_2 = 0.75$.

distancing is practiced. For example, practicing moderate social distancing ($\eta = 0.75$) and mask-wearing will not be effective in halting the spreading for any value of R_0 above 2.5 in case the efficacy of masks is limited to a reduction in the transmission without extra protection ($\alpha_1 = 0.5$ and $\alpha_2 = 1$) [Fig. 5(c)]. On the other hand, highly efficacious masks ($\alpha_1 = 0.25$ and $\alpha_2 = 0.75$) [Fig. 5] and intermediate social distancing ($\eta = 0.5$) are sufficient to prevent an epidemic outbreak for any selection of R_0 from 1 to 4, provided that at least a fraction $\beta = 0.8$ of the population follows public health measures.

B. Comparison to the ongoing pandemic

Here, we demonstrate how the proposed model can be utilized on real-world data. Specifically, we focus on the current state of the pandemic in the USA, offering evidence for the critical need of widespread adherence to public health measures to combat the spreading. First, we infer the value of η for each of the 50 US states along with the District of Columbia, by using cellphone mobility data from IHME at the University of Washington[42] (Fig. 2). The latter quantifies the extent to which the entire population reduce their mobility with respect to baseline. We hypothesize that this overall reduction is attributed only to the fraction of the population β who follows public health measures (both mask-wearing and activity reduction). Hence, the overall mobility is reduced as more people practice social distancing; with a simple rule of mixture, we can express the mobility on the vertical axis of Fig. 2 as $\eta\beta + (1 - \beta)$, which accounts for the fact that only a fraction β of the population reduces their activity by η. We then leverage this consideration to infer the state-level activity reduction η. In the $\beta - \eta$ plane of Fig. 6(a), we plot each of the 50 US states along with the District of Columbia according to their estimated activity reduction and fraction of people who regularly wear masks. In the same plane, we also report epidemic thresholds computed from Eq. (16) for different values R_0 ranging from 2 to 4 in steps of 0.5, using the optimistic estimation of mask efficacy ($\alpha_1 = 0.25$ and $\alpha = 0.75$).

For any choice of R_0, several states seem to be within the instability region, that is, above the epidemic threshold. States in the Mid-West (like Wyoming, South Dakota, and North Dakota) that engage in comparatively less mask-wearing and social distancing should achieve an epidemic outbreak according to model predictions. On the other hand, states in the North-East (like New

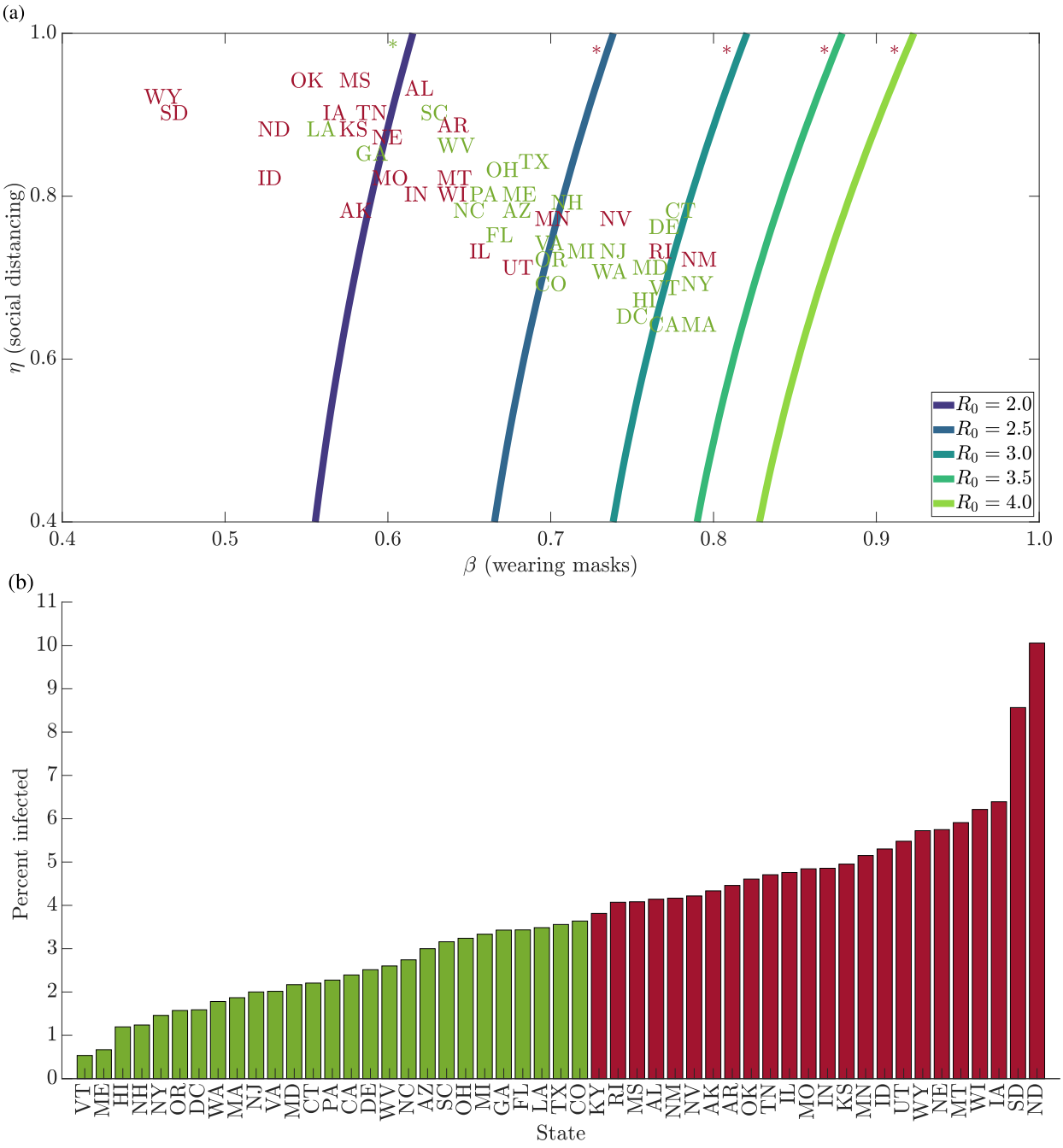

FIG. 6. Real-world analysis of the association between COVID-19 spreading in the USA and adherence to public health measures. (a) Distribution of states in the β–η plane, against threshold loci for different values of R_0; (b) *k*-means clustering of states in two groups, according to the per capita rate of cases. (a) US states along with the District of Columbia ordered in the β–η plane. The curves representing epidemic thresholds for equidistant values of R_0 between 2 and 4 with $\alpha_1 = 0.25$ and $\alpha_2 = 0.75$, computed according to Eq. (16). States are colored as a function of the number of cases per capita they experienced since July 14, 2020 (red: group associated with a high percentage of cases, and green: group associated with a low percentage of cases, according to a *k*-means analysis). A colored (red or green) asterisk close to an epidemic threshold identifies a significant difference of the mean of the corresponding group with respect to the threshold. (b) US states along the District of Columbia ordered by cumulative case count between July 14, 2020 and December 10, 2020 as a percent of the total population, according to data collected from the New York Times.[49] Red and green groups are identified based on *k*-means clustering.

York, Connecticut, and Massachusetts) or California that have been severely hit by the pandemic in Spring 2020 and have then followed more strictly public health guidelines are predicted to be below the epidemic threshold for values of R_0 of 3 or below. A clear insight, which confirms intuition and empirical observations, emerges from the analysis of these results: strong adherence to social distancing and wearing masks would take population away from the risk of an outbreak, even for high values of the reproductive parameter R_0.

Toward acquiring some statistical confidence in the predicted association between adherence to public health measures and COVID-19 spreading, we examine the cumulative cases per capita between July 14, 2020, when the CDC first officially recommended the use of masks,[24] and December 10, 2020 (date of completion of this study) according to data collected from the New York Times[49] [Fig. 6(b)]. We pursue a k-means cluster analysis that partitions states (including the District of Columbia) into two groups as a function of the sole per capita infection rate: those which experienced a high level of per capita cases (red group) and those which experienced a low number of per capita cases (green group) from July 14 to date [Fig. 6(b)].

Should we know the exact value of R_0 and should the model beget exact predictions, we would observe all the red states lying above the threshold, and the green ones below. Our results are in qualitative agreement with such a consideration for each value of R_0. To quantitatively confirm this observation, for each value of R_0 and each epidemic threshold, we test whether a group is equally distributed with respect to the threshold using a t-test. Specifically, we assign to each state a $+1$ or -1 if they are below or above the threshold and test whether the sum of these values is greater than zero for the red group or less than zero for the green group. The proposed one-dimensional statistical test is expected to be adequate for the uneven distribution of the states with respect to β and η, as it assigns a single score to each state with respect to the thresholds. For $R_0 = 2$, we reject the null hypothesis for the green group ($R_0 = 2$, $t_{26} = 12.5$, and $p < 0.001$), and for any value of R_0 above 2.5, we reject the null hypothesis for red group ($R_0 \geq 2.5$, $t_{23} < -4.3$, and $p < 0.001$). Hence, states that experienced a high per capita rate of infected individuals, marked in red in Figs. 6(a) and 6(b), are likely above the predicted epidemic threshold for a wide range of values of R_0. On the other hand, states that have experienced a low per capita rate of infected individuals, marked in green in Figs. 6(a) and 6(b), are below the epidemic threshold even for small values of R_0. Our analysis suggests that the proposed model has predictive power in discerning the effect of adherence to public health measures on epidemic spreading.

V. CONCLUSIONS

In this study, we put forward a mathematical model to probe the effectiveness of non-pharmaceutical interventions on the spreading of COVID-19. Specifically, we seek to examine how a partial adoption of social distancing and mask-wearing by only a sub-population influences the spreading of the epidemic in the entire population. Our modeling approach is based on the paradigm of activity-driven networks (ADNs), which allows for capturing the co-evolution of the network of contacts and the epidemic spreading. COVID-19 progression is described within a susceptible–exposed–infected–removed (SEIR) model that has been previously calibrated on real-world data.

To describe differential adherence to public health measures, we partition the population into two sub-populations: one that practices social distancing and wears masks and another that does not do either. Within the ADN-paradigm, social distancing is simply captured by reducing individuals' activity, so that they would generate less contacts in time. Mask-wearing is modeled by including two factors, quantifying the extent to which masks protect those who wear them and reduce the transmission of the virus from those who wear them to those who do not. Via a mean-field asymptotic approximation that retains the network heterogeneity, we establish a transparent, analytical expression for the epidemic threshold as a function of the control parameters. Numerical simulations are conducted to validate the result and shed more light into the epidemic spreading.

Overall, the model demonstrates that neither social distancing nor mask-wearing alone are likely sufficient to halt the spreading of COVID-19, unless almost the entirety of the population adheres to them. Combining the two approaches could lead to achievable scenarios in which the adherence of the majority of the population to such public health measures would suffice to combat the spreading. Comparing with real-world data on COVID-19 in the USA, we observe a close correspondence between the extent to which states comply with social distancing and mask-wearing and the local severity of the epidemic. States that are suffering from the largest number of infections are also those that comply less with public health guidelines, thereby falling well above the epidemic threshold predicted by our model.

This promising comparison with real-world data warrants several considerations. First, we cannot exclude that multiple factors contribute to the values of the model parameters, α_1, α_2, and η, beyond those related to masks and social distancing. For example, improved hygiene, reduced hand-shaking, and confinement measures could all contribute to these parameters, thereby confounding the precise inference of mask-wearing and social distancing. Second, while the proposed model is designed to capture differential responses to public health measures, it only considers homogeneous interactions within the population. This is likely not the case; it is reasonable to expect that people who follow public health guidelines are more likely to interact with others who follow public health guidelines and vice versa. This can be incorporated into the model by considering ADN with attractiveness.[39] Third, in its present incarnation, the model assumes that individuals have a preassigned tendency to adhere to public health measures, which does not change in time, due to their contacts or infection status. The current model can be extended to include behavioral changes following Refs. 35 and 50. Fourth, the transmission and progression model adopted is a simplified version of COVID-19. It, therefore, offers limited mechanical adequacy with respect to several factors, such as the incubation period, uniform transition rates to the removed state, and age-dependent parameters.[51] However, we believe that the proposed model offers a valuable tradeoff between reproduction of the salient phenomena of the epidemic spreading and its mathematical tractability and computational burden.

In the present model, social distancing is achieved by consistently scaling down the activity potential of a sub-population; a variant of the model may contemplate reducing the value of the connectivity parameter m. Another potential generalization of the model could address the drawbacks of public health measures. For example, not only does social distancing lead to societal problems such as loneliness, depression, and financial struggles,[12,14] but it also is not an option for many individuals.[52] By expanding the model to include these drawbacks, we could find an optimal balance of social distancing and still prevent epidemic outbreaks.

Overall, this work adds to the literature of mathematical treatment of the combined effect of non-pharmaceutical interventions. Beyond the study of epidemic spreading, our modeling framework finds application in diffusion processes over temporal networks where heterogeneity among sub-populations cannot be ignored.

AUTHORS' CONTRIBUTIONS

M.P. and A.R. designed and supervised the research. B.M.B. performed analytical derivations and the numerical simulations and wrote a first, preliminary draft of the manuscript. M.P. and A.R. wrote the initial submission of the manuscript, revised the manuscript based on the comments of the anonymous reviewers, and prepared the final version of the work. All the authors reviewed and approved the final version.

ACKNOWLEDGMENTS

This work was supported by the National Science Foundation (NSF) (Nos. CMMI-1561134 and CMMI-2027990) and by Compagnia di San Paolo.

APPENDIX: SENSITIVITY ANALYSIS

Here, we report the results of a sensitivity analysis executed on the results of Sec. IV A. We assess the effect of variations of parameters γ and m on the dependence of the steady-state fraction of removed individuals, R^{∞}/N, on the proportion of the population who comply with public health measures, β, and the reproduction rate, R_0. Based on the typical range for γ and m reported in the literature, we conducted a sensitivity analysis on Fig. 5 ($\gamma = 2.1$ and $m = 20$), considering the following four cases: (a) $\gamma = 2.05$ and $m = 20$; (b) $\gamma = 2.15$ and $m = 20$; (c) $\gamma = 2.1$ and $m = 18$; and (d) $\gamma = 2.1$ and $m = 22$. Simulation results illustrated in Fig. 7 suggest that our claims are robust with respect to parameter variations within 5%–10% of their nominal value.

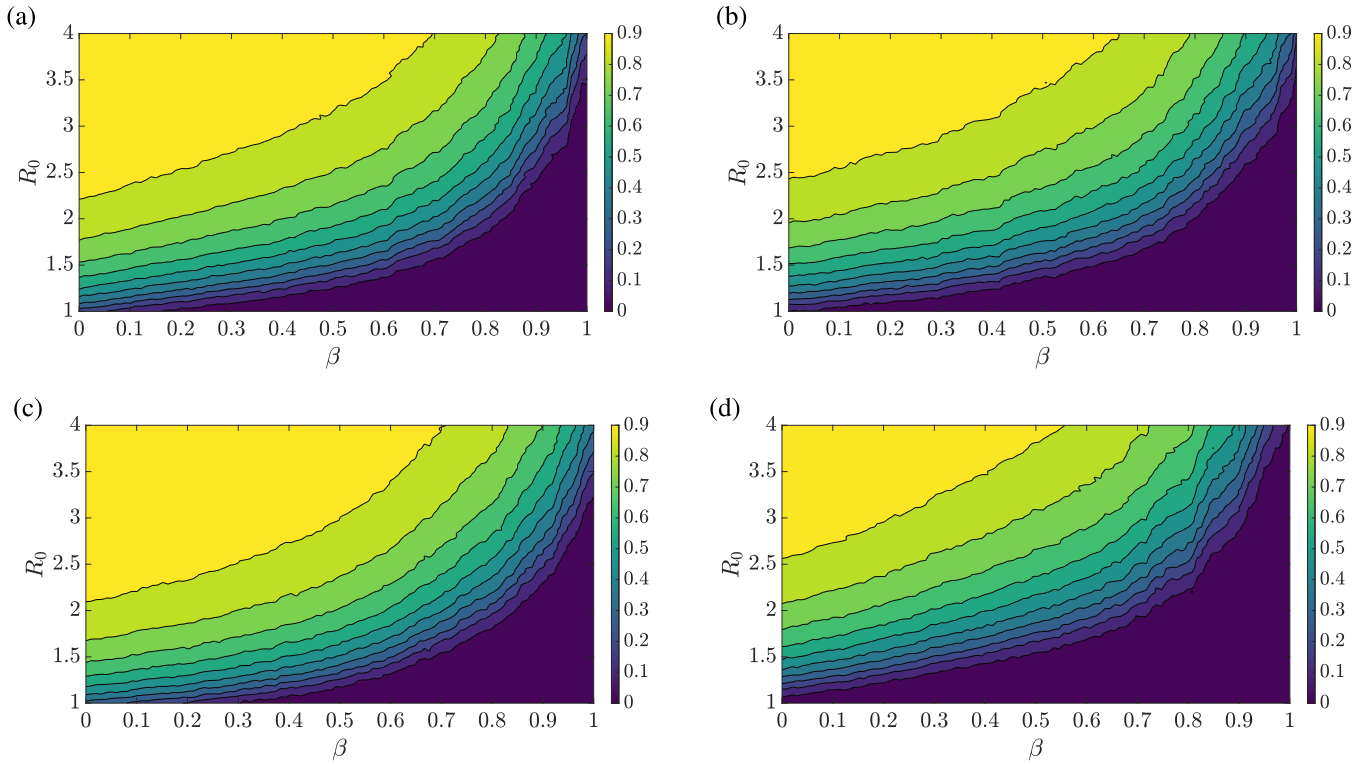

FIG. 7. Sensitivity analysis of the dependence of the steady-state fraction of removed individuals, R^{∞}/N (color coded), on β and R_0. Each panel covers different combinations of γ and m: (a) $\gamma = 2.05$ and $m = 20$, (b) $\gamma = 2.10$ and $m = 18$, (c) $\gamma = 2.15$ and $m = 20$, and (d) $\gamma = 2.15$ and $m = 22$. Remaining parameters are set as in Fig. 5 ($\eta = 0.25$, $\alpha_1 = 1$, and $\alpha_2 = 1$). (a) $\gamma = 2.05$ and $m = 20$, (b) $\gamma = 2.10$ and $m = 18$, (c) $\gamma = 2.15$ and $m = 20$, and (d) $\gamma = 2.15$ and $m = 22$.

DATA AVAILABILITY

The data that support the findings of this study are available within the article.

REFERENCES

[1] J. B. Nuzzo, L. Mullen, M. Snyder, A. Cicero, and T. V. Inglesby, *Preparedness for a High Impact Respiratory Pathogen Pandemic* (The Johns Hopkins Center for Health Security, 2019), p. 84.
[2] Centers for Disease Control and Prevention, "1918 pandemic (H1N1 virus)," see https://www.cdc.gov/flu/pandemic-resources/1918-pandemic-h1n1.html (last accessed March 11, 2020).
[3] R. D. Smith, "Responding to global infectious disease outbreaks: Lessons from SARS on the role of risk perception, communication and management," Soc. Sci. Med. **63**, 3113–3123 (2006).
[4] R. J. de Groot, S. C. Baker, R. S. Baric, C. S. Brown, and C. Drosten, Enjuanes, "Commentary: Middle East respiratory syndrome coronavirus (MERS-CoV): Announcement of the coronavirus study group," J. Virol. **87**, 7790–7792 (2013).
[5] Centers for Disease Control and Prevention, "Summary of probable SARS cases with onset of illness," see https://www.who.int/health-topics/severe-acute-respiratory-syndrome (last accessed March 11, 2020).
[6] World Health Organization, "Eastern Mediterranean Region," see http://www.emro.who.int/health-topics/mers-cov/mers-outbreaks.html (last accessed March 11, 2020).
[7] World Health Organization, "WHO coronavirus disease (COVID-19) dashboard," see https://COVID19.who.int (last accessed March 11, 2020).
[8] R. Zhang, Y. Li, A. L. Zhang, Y. Wang, and M. J. Molina, "Identifying airborne transmission as the dominant route for the spread of COVID-19," Proc. Natl. Acad. Sci. U.S.A. **117**, 14857–14863 (2020).
[9] E. L. Anderson, P. Turnham, J. R. Griffin, and C. C. Clarke, "Consideration of the aerosol transmission for COVID-19 and public health," Risk Anal. **40**, 902–907 (2020).
[10] J. Wang and G. Du, "COVID-19 may transmit through aerosol," Ir. J. Med. Sci. **189**, 1143 (2020).
[11] D. K. Chu, E. A. Akl, S. Duda, K. Solo, S. Yaacoub, H. J. Schünemann, D. K. Chu, and E. A. Akl, "Physical distancing, face masks, and eye protection to prevent person-to-person transmission of SARS-CoV-2 and COVID-19: A systematic review and meta-analysis," Lancet **395**, 1973–1987 (2020).
[12] E. Caroppo, P. De Lellis, I. Lega, A. Candelori, D. Pedacchia, A. Pellegrini, R. Sonnino, V. Venturiello, M. Ruiz Marìn, and M. Porfiri, "Unequal effects of the national lockdown on mental and social health in Italy," Ann. Istituto Super. Sanità **56**, 497–501 (2020).
[13] S. K. Brooks, R. K. Webster, L. E. Smith, L. Woodland, S. Wessely, N. Greenberg, and G. J. Rubin, "The psychological impact of quarantine and how to reduce it: Rapid review of the evidence," Lancet **395**, 912–920 (2020).
[14] I. F. Tso and S. Park, "Alarming levels of psychiatric symptoms and the role of loneliness during the COVID-19 epidemic: A case study of Hong Kong," Psychiatry Res. **293**, 113423 (2020).
[15] L. Matrajt and T. Leung, "Evaluating the effectiveness of social distancing interventions to delay or flatten the epidemic curve of coronavirus disease," Emerging Infect. Dis. **26**, 1740–1748 (2020).
[16] A. D. Wiese, J. Everson, and C. G. Grijalva, "Social distancing measures: Evidence of interruption of seasonal influenza activity and early lessons of the SARS-CoV-2 pandemic," Clin. Infect. Diseases **2020**, ciaa834.
[17] S. J. Olsen, E. Azziz-Baumgartner, A. P. Budd, L. Brammer, S. Sullivan, R. F. Pineda, C. Cohen, and A. M. Fry, "Decreased influenza activity during the COVID-19 pandemic—United States, Australia, Chile, and South Africa, 2020," Morbidity Mortality Weekly Rep. **69**, 1305–1309 (2020).
[18] E. Estrada, "COVID-19 and SARS-CoV-2. Modeling the present, looking at the future," Phys. Rep. **869**, 1–51 (2020).
[19] F. Parino, L. Zino, M. Porfiri, and A. Rizzo, "Modelling and predicting the effect of social distancing and travel restrictions on COVID-19 spreading," J. R. Soc. Interface **18**, 20200875 (2021).
[20] M. Mancastroppa, R. Burioni, V. Colizza, and A. Vezzani, "Active and inactive quarantine in epidemic spreading on adaptive activity-driven networks," Phys. Rev. E **102**, 020301(R) (2020).
[21] C. N. Ngonghala, E. Iboi, S. Eikenberry, M. Scotch, C. R. MacIntyre, M. H. Bonds, and A. B. Gumel, "Mathematical assessment of the impact of non-pharmaceutical interventions on curtailing the 2019 novel coronavirus," Math. Biosci. **325**, 108364 (2020).
[22] A. Aleta, D. Martín-Corral, A. Pastore y Piontti, M. Ajelli, M. Litvinova, M. Chinazzi, N. E. Dean, M. E. Halloran, I. M. Longini, S. Merler, A. Pentland, A. Vespignani, E. Moro, and Y. Moreno, "Modelling the impact of testing, contact tracing and household quarantine on second waves of COVID-19," Nature Human Behav. **4**, 964 (2020).
[23] P. C. Silva, P. V. Batista, H. S. Lima, M. A. Alves, F. G. Guimarães, and R. C. Silva, "COVID-ABS: An agent-based model of COVID-19 epidemic to simulate health and economic effects of social distancing interventions," Chaos, Solitons Fractals **139**, 110088 (2020).
[24] Centers for Disease Control and Prevention, "CDC calls on Americans to wear masks to prevent COVID-19 spread," see https://www.cdc.gov/media/releases/2020/p0714-americans-to-wear-masks.html (last accessed March 11, 2020).
[25] N. H. Leung, D. K. Chu, E. Y. Shiu, K. H. Chan, and J. J. M. Hau, "Respiratory virus shedding in exhaled breath and efficacy of face masks," Nat. Med. **26**, 676–680 (2020).
[26] A. Konda, A. Prakash, G. A. Moss, M. Schmoldt, G. D. Grant, and S. Guha, "Aerosol filtration efficiency of common fabrics used in respiratory cloth masks," ACS Nano **14**, 6339–6347 (2020).
[27] M. Gandhi, C. Beyrer, and E. Goosby, "Masks do more than protect others during COVID-19: Reducing the inoculum of SARS-CoV-2 to protect the wearer," J. Gen. Intern. Med. **35**, 3063 (2020).
[28] W. Lyu and G. L. Wehby, "Community use of face masks and COVID-19: Evidence from a natural experiment of state mandates in the US," Health Aff. **39**, 1419–1425 (2020).
[29] R. O. J. H. Stutt, R. Retkute, M. Bradley, C. A. Gilligan, and J. Colvin, "A modelling framework to assess the likely effectiveness of facemasks in combination with 'lock-down' in managing the COVID-19 pandemic," Proc. R. Soc. Lond. A. Math. Phys. Sci. **476**, 20200376 (2020).
[30] D. Kai, G.-P. Goldstein, A. Morgunov, V. Nangalia, and A. Rotkirch, "Universal masking is urgent in the COVID-19 pandemic: SEIR and agent based models, empirical validation, policy recommendations," arXiv:2004.13553 (2020).
[31] D. N. Fisman, A. L. Greer, and A. R. Tuite, "Bidirectional impact of imperfect mask use on reproduction number of COVID-19: A next generation matrix approach," Infect. Disease Model. **5**, 405–408 (2020).
[32] Y. Tian, A. Sridhar, O. Yagan, and H. V. Poor, "Analysis of the impact of mask-wearing in viral spread: Implications for COVID-19," arXiv:2011.04208 (2020).
[33] N. Perra, B. Gonçalves, R. Pastor-Satorras, and A. Vespignani, "Activity driven modeling of time varying networks," Sci. Rep. **2**, 2045–2322 (2012).
[34] S. Liu, N. Perra, M. Karsai, and A. Vespignani, "Controlling contagion processes in activity driven networks," Phys. Rev. Lett. **112**, 118702 (2014).
[35] A. Rizzo, M. Frasca, and M. Porfiri, "Effect of individual behavior on epidemic spreading in activity-driven networks," Phys. Rev. E **90**, 042801 (2014).
[36] A. Rizzo, B. Pedalino, and M. Porfiri, "A network model for Ebola spreading," J. Theor. Biol. **394**, 212–222 (2016).
[37] A. Rizzo and M. Porfiri, "Innovation diffusion on time-varying activity driven networks," Eur. Phys. J. B **89**, 1–8 (2016).
[38] L. Zino, A. Rizzo, and M. Porfiri, "Consensus over activity-driven networks," IEEE Trans. Control Netw. Syst. **7**, 866–877 (2020).
[39] I. Pozzana, K. Sun, and N. Perra, "Epidemic spreading on activity-driven networks with attractiveness," Phys. Rev. E **96**, 042310 (2017).
[40] A. L. Barabási, "The origin of bursts and heavy tails in human dynamics," Nature **435**, 1476–4687 (2005).
[41] H.-H. Jo, M. Karsai, J. Kertész, and K. Kaski, "Circadian pattern and burstiness in mobile phone communication," New J. Phys. **14**, 013055 (2012).
[42] Institute for Health Metrics and Evaluation (IHME), "COVID-19 projections," see https://COVID19.healthdata.org/projections (last accessed March 11, 2020).
[43] L. Peeples, "Face masks: What the data say," Nature **586**, 186 (2020).
[44] J. Howard, A. Huang, Z. Li, and A. Rimoin, "Face masks against COVID-19: An evidence review," Proc. Natl. Acad. Sci. U.S.A. **118**(4), e2014564118 (2021).

[45]J. Yan, S. Guha, P. Hariharan, and M. Myers, "Modeling the effectiveness of respiratory protective devices in reducing influenza outbreak," Risk Anal. **39**, 647–661 (2019).
[46]M. J. Hendrix, C. Walde, K. Findley, and R. Trotman, "Absence of apparent transmission of SARS-CoV-2 from two stylists after exposure at a hair salon with a universal face covering policy in Springfield, Missouri, May 2020," Morbidity Mortality Weekly Rep. **69**, 930 (2020).
[47]The reproduction number is the number of secondary cases in an entirely susceptible population from a single infected node.
[48]B. Rahman, E. Sadraddin, and A. Porreca, "The basic reproduction number of SARS-CoV-2 in Wuhan is about to die out, how about the rest of the world?" Rev. Med. Virol. **30**, e2111 (2020).
[49]The New York Times, "COVID-19 data," see https://github.com/nytimes/COVID-19-data (last accessed March 11, 2020).
[50]L. Zino, A. Rizzo, and M. Porfiri, "Modeling memory effects in activity-driven networks," SIAM J. Appl. Dyn. Syst. **17**, 2830–2854 (2018).
[51]A. Truszkowska, B. Behring, J. Hasanyan, L. Zino, S. Butail, E. Caroppo, Z.-P. Jiang, A. Rizzo, and M. Porfiri, "High-resolution agent-based modeling of COVID-19 spreading in a small town," Adv. Theory Simulat. **4**(3), 2000277 (2021).
[52]J. A. Weill, M. Stigler, O. Deschenes, and M. R. Springborn, "Social distancing responses to COVID-19 emergency declarations strongly differentiated by income," Proc. Natl. Acad. Sci. U.S.A. **117**, 19658–19660 (2020).